Civil Engineering Infrastructures Journal xx,xx

DOI: 10.22059/ceij.2025.383680.2170

Seismic Performance Assessment of Steel Concentrically Braced Frames (CBFs) Equipped with Crescent-shaped Braces (CSBs)

#	Name	Email Address	Degree	Position	Country	Affiliation
1	Asghari, Abazar	abazar.asghari@ut.ac.ir	Ph.D.	Associate Professor		School of Civil Engineering, College of Engineering, University of Tehran, Tehran, Iran.
2	Tajik, Nima	nimataji@buffalo.edu	Ph.D. Candidate	Other	United States of America	Department of Civil, Structural and Environmental Engineering, State University of New York at Buffalo, Buffalo, NY, USA

Received: 26/10/2024

Revised: 19/05/2025

Accepted: 24/05/2025

Abstract

This paper focuses on studying the elastic and inelastic behavior of steel concentrically braced frames (CBFs) with crescent-shaped braces (CSBs) and proposes a novel seismic design approach due to the lack of existing seismic specifications. The results of the elastic analyses demonstrate a reduction in the lateral stiffness of the frame as the arm (ξ) increases. Specifically, when ξ reaches approximately one fifth of the length of the braced member, the lateral stiffness of braced frames becomes nearly equal to that of moment-resisting frames. The analysis results further verify that the strength and stiffness of braced members are not inherently coupled. The findings highlight that by specifying the appropriate value of ξ (arm length), the desired stiffness can be achieved. This implies the conventional concentrically braced members typically lack such a specification. Nonlinear analyses of braced frames confirm that frames braced with CSBs can be classified as Steel Special Concentrically Braced Frames (SCBFs) rather than ordinary concentrically braced frames (OCBFs). Nonlinear analysis indicates the response modification factor for this type of frame should be 3.5. Additionally cyclic behavior of frames braced with CSBs indicated that by increasing the value of ξ, more energy dissipation can be achieved during earthquake loading.

Keywords: Curved Crescent-shaped brace, Reduction factor, Curved Crescent-shaped braced frame, Push over analysis, Response modification factor, Cyclic behavior

1. Introduction

Typically, the initial design process for most building structures relies on equivalent static loads as prescribed by the building design guidelines. The vertical distribution of these static loads appears to be primarily determined by the elastic vibration modes of the structure. However, structures do not remain in an elastic state during severe earthquakes; they are expected to undergo significant nonlinear deformations. This poses a significant challenge in the design of buildings, as traditional design practices are typically based on the assumption of elastic vibrations [Jaberi and Asghari, 2022; Jaberi and Asghari, 2020a; Jaberi et al., 2024; Fanaie et al., 2024]. One of the most recent advancements in earthquake engineering is the adoption of a new design approach known as Performance-Based Seismic Design (PBSD) [Özuygur, 2016]. Despite its origins dating back to the late 20th century, this method has gained significant popularity in recent years. Indeed, Performance-Based Seismic Design (PBSD) is a relatively new approach in the seismic design of buildings. This method has been developed to enhance the performance of structures when subjected to severe earthquake loadings. The efficiency and effectiveness of the PBSD method serve as the primary motivations behind its development [Shirpour and Fanaie, 2024; Asghari and Gandomi, 2016]. The philosophy underlying Performance-Based Seismic Design (PBSD) of buildings is to define and specify the components of a structure, including materials, section shapes and dimensions, connection details, and other relevant factors, based on their expected behavior during predefined earthquakes. In many design guidelines that employ a performance-based design approach, the process begins by establishing the objectives and desired performance levels for the building. Once these performance objectives are defined, specific design specifications are proposed to ensure that the building meets the predefined performance criteria. As the objectives of seismic design are expressed more accurately and clearly, and the proposed guidelines are defined more appropriately to meet those objectives, it can be said with greater certainty that the designed buildings will fulfill the intended objectives and expected performance. The proposed guidelines should be based on the actual behavior of the building during earthquakes and should encompass all essential structural requirements. Although performance-based design is considered a reliable approach for designing building structures, it is relatively time-consuming and iterative in nature. As a result, this method is rarely used in the design of building structures nowadays, and the design of most building structures is generally based on prescribed forces and their elastic behavior. This research does not aim to examine the design details of this method and does not address it [Steneker et al., 2020; Mohammadgholipour and Billah, 2024].

Currently, steel moment frames (SMFs), steel ordinary concentrically braced frames (CBFs), steel eccentrically braced frames (EBFs), steel special plate shear walls, special reinforced concrete shear walls, and steel moment frames with either concentric or eccentric bracing are recognized as the most well-known and commonly used structural systems for seismic resistance against earthquake forces [Jalilzadeh Afshari et al., 2019; Asghari and Azimi Zarnagh, 2017; Rezaee and Asghari, 2024; Tajik et al., 2024; Tajik et al., 2025a; Tajik et al., 2025b; Mesr Habiby and Behnamfar, 2023; Bypour et al., 2024; Tajik et al., 2025c, Mahmoudian et al., 2024]. Many studies have used these systems for comparison with newly developed systems [Aydin et al., 2012; Aydin et al., n.d.; Aydin et al., 2019].

Although SMFs have high ductility, their lower stiffness makes them less economical for relatively tall buildings [Asghari and Saharkhizan, 2019; Asghari and Azimi, 2017; Jaberi and Asghari, 2020b]. OCBFs are indeed one of the long-standing seismic resistance structural systems that have been utilized by structural designers for many years. Figure 1 illustrates the common configurations of this type of structural system. Generally, the selection of OCBFs' configuration is based on the lateral load magnitude, required level of ductility, and architectural-aesthetic requirements [Izadinia et al., 2012]. In the design and detailing of OCBFs, it is common to consider moment-resisting connections between the bracing members and beams or columns. Additionally, in some cases, a combination of moment frames with concentric bracing is used to reduce drift in building frames [Sabelli, 2001].

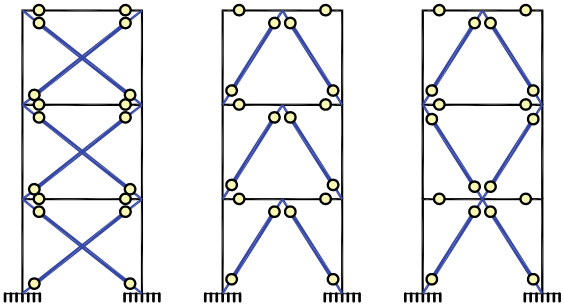

Fig. 1. Common configurations for concentrically braced frames

One of the main concerns in such structural systems is the buckling of the bracing members and consequently the reduction in the ductility of these structural systems [Shirpour et al., 2024; Bastami and Ahmady Jazany, 2019]. Extensive studies have been conducted in the past to prevent the buckling of bracing members and to increase the ductility of such structural systems. For example, using buckling-restrained braces (BRB) improves the seismic performance of such structural systems significantly compared to conventional concentric braces [Yuan et al., 2022; Wang et al., 2019; Asghari, 2016a]. In line with the results obtained from research conducted on such structural systems, design codes and regulations have also improved the behavior of these types of structural systems by introducing additional requirements. For example, the AISC-341-22, states that the design of beams and columns should not be based on forces less than those resulting from the following analyses [AISC, 2022]:

(a) An analysis in which it is assumed that the tensile force of braces which are in tension is equal to $R_yF_yA_g$ and the compression force of braces which are in compression is equal to $1.14F_{cre}A_g$.

(b) An analysis in which it is assumed that the tensile force of braces which are in tension is equal to $R_yF_yA_g$ and the compression force of braces which are in compression is equal to $0.3\times1.14F_{cre}A_g$. Where: A_g is gross cross-sectional area of braced member. F_y is yield stress of used steel. R_y is the proportion of expected yield stress of steel to determined minimum yield stress of steel. F_{cre} Expected compressive stress due to buckling.

Generally, a suitable structural system is a system that meets the multiple objectives (stiffness, strength and ductility) simultaneously and to the desired extent, which can be expressed as a curve based on lateral force and lateral deformation. This curve is usually called the target curve. The curve can indicate the lateral stiffness (elastic behavior), yield strength and overall ductility (inelastic behavior), cyclic behavior and hardening behavior. Unfortunately, Concentrically braced frames with diagonal elements have different behavior curves from the target curve; because such bracing systems have very high stiffness, but they have lower strength and this is one of the prominent weaknesses of such structural systems. Therefore, in order to improve the seismic performance of these structural systems and to bring their response curve closer to the target curve, it is necessary to add members with adjustable stiffness and strength to these structural systems. For this purpose, Palermo and his colleagues [Palermo et al., 2015] were able to obtain a lateral load-resisting system with adjustable stiffness and strength by introducing braces with curved members referred to as crescent shaped braces, (CSBs), as shown in Figure 2.

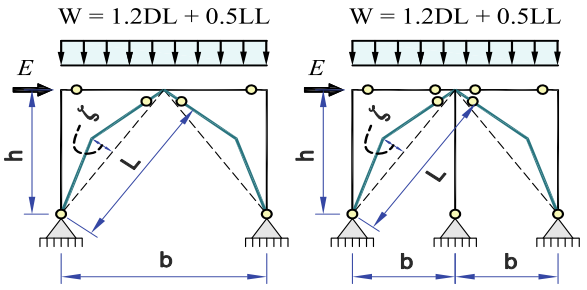

(a) (b)

Fig. 2. Crescent shaped braced frame introduced by Palermo etc. (a) The double bilinear symmetric configuration of the CSB, (b) two mirrored disposed bilinear configurations of the CSB

Palermo and his colleagues in their research on a one-story frame showed that CSBs, while having the ability to adjust stiffness and strength, if used in tension and compression (in a complementary way), they will have very high hysteresis energy dissipation and based on numerical and experimental results, their ductility coefficient will be between 3 and 3.5. Omar Koma and his colleagues also showed that unlike ordinary concentrically braces, CSBs when subjected to compressive force, will not exhibit sudden buckling and this is due to the special shape of this type of braces. Of course, to prevent buckling outside the frame plane, choosing the appropriate shape for the brace section and also fixing the connection of the two ends of the brace for buckling outside the frame plane is very necessary.

As observed from the history of past research, it seems that so far only the ductility of bilinear symmetric configuration of the CSB has been addressed as a lateral load-resisting member, and the overall behavior of steel frames in conjunction with these types of braces has received less

attention, so in this research an attempt will be made to study the overall behavior of building frames in conjunction with CSBs through a parametric study. For this purpose, three frames of 3, 6 and 9 stories have been selected with seven different configurations (ξ=L/4 ،ξ=L/6 ،ξ=L/8 ، ξ=L/10 ،ξ=L/15 ،ξ=L/20 ،ξ=L/30). The elastic and inelastic behavior of these frames has been studied using linear and nonlinear static (pushover) and nonlinear time history analysis.

2. Evaluation of elastic behavior of CSBs

Crescent-shaped braces are members that provide more freedom of action to adjust stiffness and resistance in building design through them. In other words, since the resistance and stiffness in crescent-shaped braces are not coupled (not involved with each other), as a result, by using them, the designer will be able to control the resistance and lateral displacement of the structure as much as necessary, in Figure 3, the lateral displacement of a crescent-shaped bracing member for different values of ξ, (ξ=L/4 ،ξ=L/6 ،ξ=L/8 ،ξ=L/10 ،ξ=L/15 ،ξ=L/20 ، ξ=L/30 ،ξ=0) is displayed for the same lateral force (P).

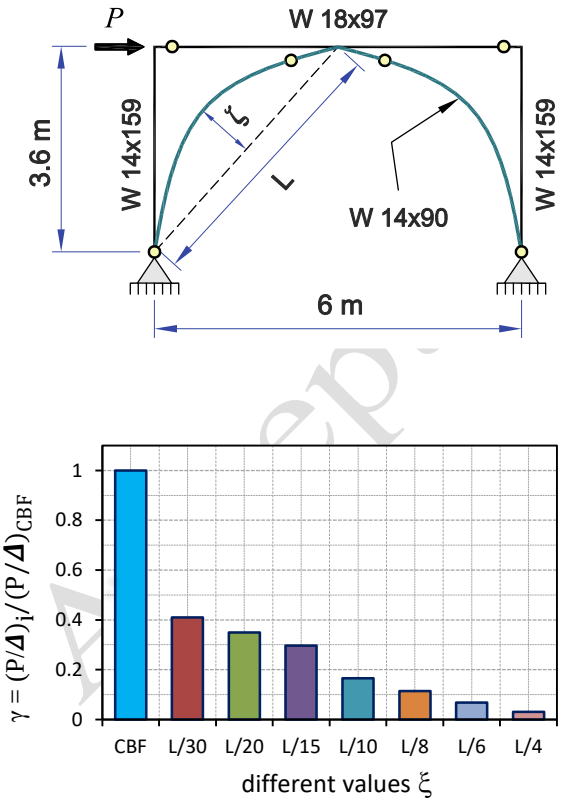

Fig. 3. Crescent bracings stiffness for different values of ξ. (ξ=L/4 ،ξ=L/6 ،ξ=L/8 ،ξ=L/10 ، ξ=L/15 ،ξ=L/20 ،ξ=L/30 ،ξ=0)

According to Figure 3, the lateral stiffness of crescent shaped braced members significantly reduces as the ξ increases, this can be very effective in adjusting the stiffness and strength of braced members, It is necessary to mention that in Figure 3, the lateral stiffness of the crescent-shaped bracing member is shown for different values of ξ, but for the same cross section of bracing member. However, in practical applications, the section of the bracing member may change for different ξ, and this issue will be considered in the next section of paper.

According to Figure 4, for the evaluation of the elastic behavior of OCBFs which are braced with CSBs, three building frames of 3, 6, and 9 stories have been chosen as case studies, each with eight different configurations (ξ=L/4, ξ=L/6, ξ=L/8, ξ=L/10, ξ=L/15, ξ=L/20, ξ=L/30, ξ=0). In addition, a moment frame with intermediate ductility has been studied for each of under studied frames to compare the results of the parametric analysis.

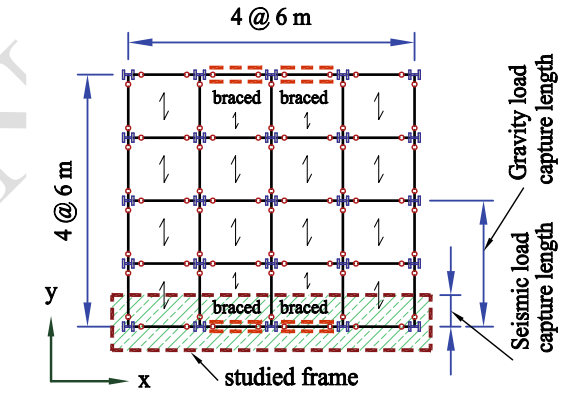

(a)

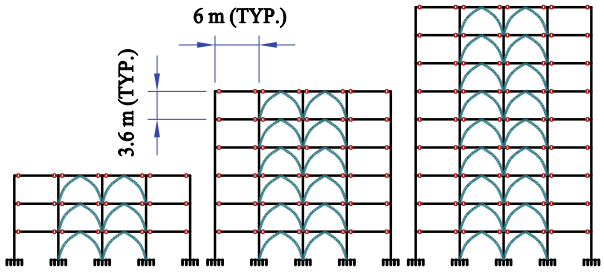

(b) (c) (d)

Fig. 4. Concentrically braced frames braced with CSBs. (a) Plan view of studied building, (b) 3 story, (c) 6 story, (d) 9 story.

The assumptions used in the analysis and design of the frames shown in Figure 4 are as follows: MRFs, CBFs, CSBFs represent moment resistant frames, concentrically braced frames, and crescent shape braced frames, respectively. Number of frame's bays is 4, length of bays is

selected to be 6 meters, the height of stories is set to be 3.6 meter and the dead and live load applied to beams are set to be 28 and 6 kN/m respectively. Seismic loading is applied according to Iranian code of practice for seismic resistant design of buildings fourth edition [Iranian code, n.d.]. Due to the characteristics of the perimeter frames investigated in this research, the columns of the seismic frames in each direction are only affected by earthquake forces acting in the same direction, and none of the columns experience multiple earthquake accelerograms simultaneously. Therefore, to reduce computational effort, 2D analyses are performed instead of 3D analyses as displayed in Figure 4-a. This approach is valid as long as the seismic frames do not interact with each other. So, the efficient seismic weight is assumed to be 4 times the applied gravity loads. Because lateral load resisting frames should also withstand the P-Δ effect of gravity load resisting frames, so for these frames, the effect of P-Δ should be increased 4 times like seismic design procedure. Analysis and design are conducted using commercial software ETABS and the LRFD method [ETABS, 1995]. For seismic design of building frames with common types of bracing, the AISC 341-22 specification is used, according to this specification, for special concentrically braced frames, required design strength of columns and beams should not be less than the following analyses:

a) Analysis in which tension and compression forces in bracing members are assumed to be $R_yF_yA_g$ and $1.14F_{cre}A_g$, respectively.
b) Analysis in which tension and compression forces in bracing members are assumed to be $R_yF_yA_g$ and $0.3\times1.14F_{cre}A_g$, respectively.

Where: A_g is the gross section of bracing member, F_y is the yield stress of used steel and R_y is the ratio of expected yield stress of steel to specified minimum yield stress of steel, F_{cre} is expected compression stress of steel due to buckling, F_{ye} is expected yield stress of steel.

3. Proposed procedure for seismic design of concentrically braced frames braced with CSBs

Because in none of designing guide lines there are no specifications for seismic design of concentrically braced frames braced with CSBs, so in this paper a procedure is introduced for seismic design of these frames. It is assumed that design strength of beams and columns should not be less than the following analysis:

(a) An analysis in which effective force of tension bracing is set to be P_{et} and the effective force of compression bracings is set to be P_{ec}.
(b) an analysis in which it is assumed that the effective force of tension bracing is set to be P_{et} and the effective force of compression bracings is set to be $0.3P_{ec}$.

As displayed in Figure 5 effective forces of P_{et} and P_{ec} are calculated using the following equations:

$$\frac{P_{et}}{R_yA_gF_y}+\frac{P_{et}\times\xi}{R_yM_p}=1 \quad (1)$$

$$\frac{P_{ec}}{R_yA_gF_{cr}}+\frac{P_{ec}\times\xi}{R_yM_p}=1 \quad (2)$$

$$P_{et}=\frac{R_y}{\left(\frac{1}{A_gF_y}+\frac{\xi}{M_p}\right)} \quad (3)$$

$$P_{ec}=\frac{R_y}{\left(\frac{1}{A_gF_{cr}}+\frac{\xi}{M_p}\right)} \quad (4)$$

Where: A_g is the gross section of the bracing, F_y is the yield stress of used steel, R_y is the ratio of expected yield stress of steel to specified minimum yield stress of steel, F_{cre} is expected compression stress of steel due to buckling, F_{ye} is expected yield stress of steel and Mp is the plastic moment of braced member.

This should be noted that according to AISC 341-22, for seismic design of OCBFs and concentrically braced frames braced with CSBs, after running basic analyses (common analyses for designing frames), firstly, bracings are omitted from the analysis model and for preventing the frames from instability the story diaphragms are districted from lateral displacement, then by applying seismic forces as shown in Figure 5 along the longitudinal direction of tension and compression bracing systems, beams and columns, they have been reanalyzed and designed in the presence of gravity loads with coefficients relevant to them in the presence of earthquake forces [Asghari, 2017; Asghari and Asadi, 2016; Asghari, 2016b]. In Figure 6, various analytical models are shown for the seismic design of concentrically braced frames braced with CSBs.

Table 1 to 3 displays the analysis results of all of studied frames and Figure 7 displays lateral displacement diagram of studied frames.

According to the capacity-limited design discussed in this section, the beams and the columns are designed for the maximum force caused by braces which act as fuses in the

investigated structures. So, the beams and the columns must remain elastic during the earthquake.

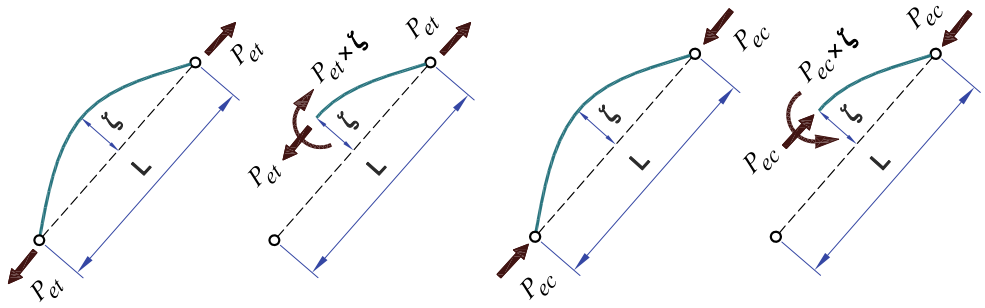

(a) (b)

Fig. 5. Effective forces of bracing members for seismic design of concentrically braced frames braced with CSBs. (a) effective force of tension braces, (b) effective force of compression braces

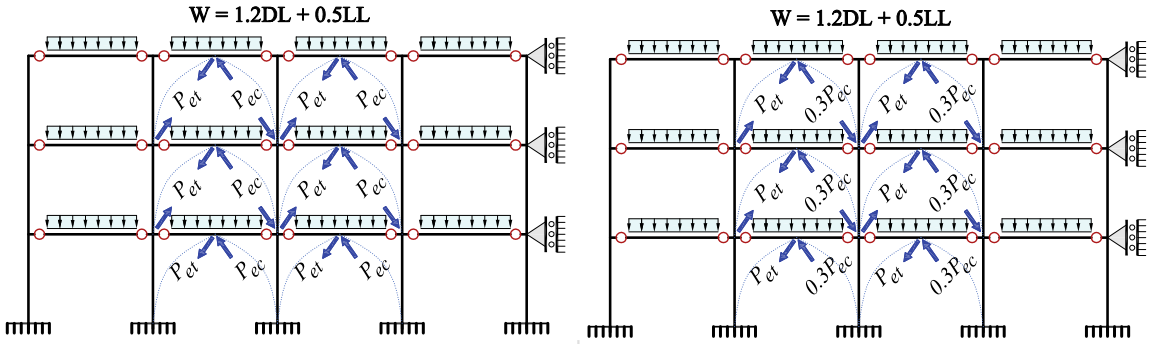

model (a) model (b)

Fig. 6. Reassessment of OCBFs braced with CSBs for seismic forces

Table 1. Elastic analysis results of 9 story studied frames

Type of Frame	C_d	T_{exp} (sec)	C_u	Δ_{roof} (cm)	T_{ana} (sec)	$C_u^* \geq 0.12AI$	$\Delta^*_{roof} = \Delta_{roof}\frac{C_u^*}{C_u}$ (cm)	$\Delta_{all} = \frac{0.02h}{C_d}$ (cm)
CBF	5	0.6790	0.1213	6.73	1.098	0.0811	4.50	12.96
$\xi = L/30$	"	"	"	12.50	1.446	0.0654	6.74	"
$\xi = L/20$	"	"	"	13.16	1.481	0.0642	6.97	"
$\xi = L/15$	"	"	"	15.70	1.673	0.0587	7.60	"
$\xi = L/10$	"	"	"	19.17	1.809	0.0555	8.77	"
$\xi = L/8$	"	"	"	24.27	2.029	0.0512	10.24	"
$\xi = L/6$	"	"	"	25.80	2.102	0.0495	11.36	"
$\xi = L/4$	"	"	"	33.60	2.448	0.0452	12.52	"
MRF	4	1.0864	0.0900	29.87	2.629	0.0475	15.77	16.20

Table 2. Elastic analysis results of 6 story studied frames

Type of Frame	C_d	T_{exp} (sec)	C_u	Δ_{roof} (cm)	T_{ana} (sec)	$C_u^* \geq 0.12AI$	$\Delta^*_{roof} = \Delta_{roof}\frac{C_u^*}{C_u}$ (cm)	$\Delta_{all} = \frac{0.02h}{C_d}$ (cm)
CBF	5	0.5010	0.1588	3.61	0.743	0.1123	2.55	8.64
$\xi = L/30$	"	"	"	7.93	1.033	0.0852	4.25	"
$\xi = L/20$	"	"	"	8.24	1.054	0.0838	4.35	"
$\xi = L/15$	"	"	"	9.38	1.167	0.0773	4.57	"
$\xi = L/10$	"	"	"	12.61	1.327	0.0699	5.55	"
$\xi = L/8$	"	"	"	14.48	1.418	0.0664	6.05	"

$\xi = L/6$	"	"	"	17.43	1.562	0.0617	6.77	"
$\xi = L/4$	"	"	"	21.93	1.782	0.0550	8.55	"
MRF	4	0.8015	0.1157	18.54	1.880	0.0594	9.52	10.80

Table 3. Elastic analysis results of 3 story studied frames

Type of Frame	C_d	T_{exp} (sec)	C_u	Δ_{roof} (cm)	T_{ana} (sec)	$C_u^* \geq 0.12AI$	$\Delta_{roof}^* = \Delta_{roof}\frac{C_u^*}{C_u}$ (cm)	$\Delta_{all} = \frac{0.025h}{C_d}$ (cm)
CBF	5	0.2979	0.1591	0.804	0.376	0.1591	0.804	5.40
$\xi = L/30$	"	"	"	3.673	0.767	0.1092	2.521	"
$\xi = L/20$	"	"	"	3.731	0.773	0.1085	2.544	"
$\xi = L/15$	"	"	"	4.222	0.868	0.0984	2.611	"
$\xi = L/10$	"	"	"	7.233	1.119	0.0799	3.632	"
$\xi = L/8$	"	"	"	6.987	1.061	0.0834	3.663	"
$\xi = L/6$	"	"	"	8.801	1.244	0.0696	4.771	"
$\xi = L/4$	"	"	"	8.895	1.233	0.0673	5.066	"
MRF	4	0.4766	0.1750	9.392	1.171	0.0848	4.551	6.75

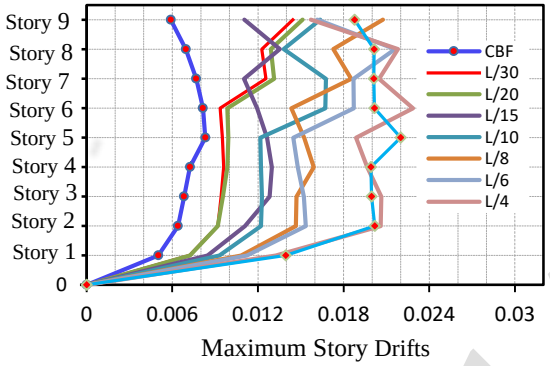

(a) Drift curves for 9 story frames

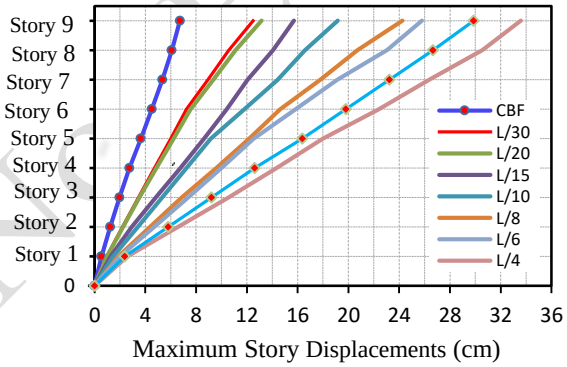

(b) maximum lateral displacement curve for 9 story frames

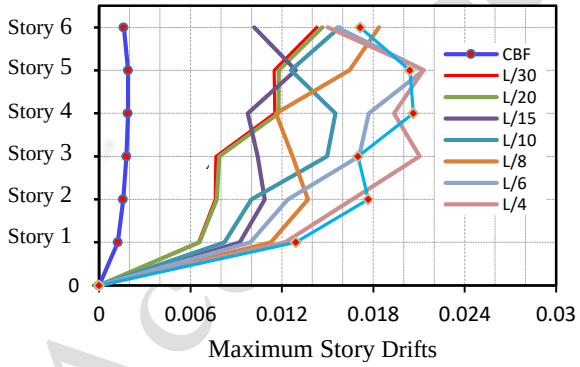

(c) Drift curves for 6 story frames

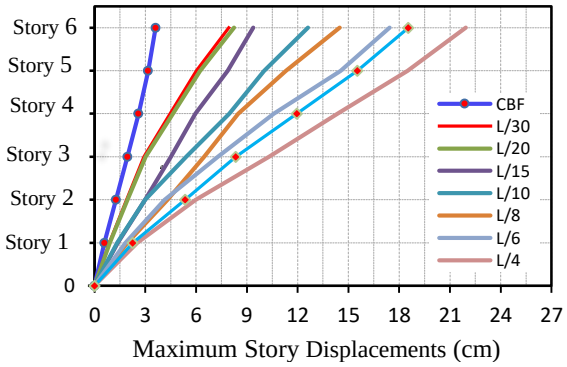

(d) maximum lateral displacement curve for 6 story frames

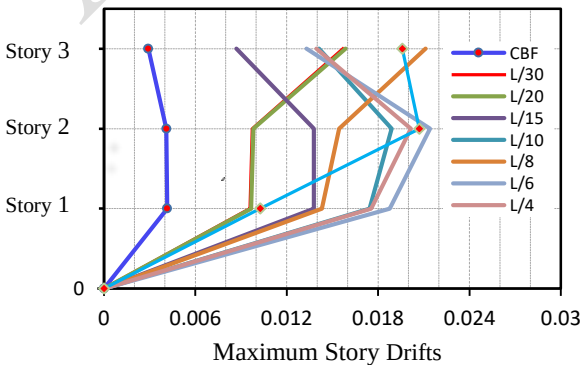

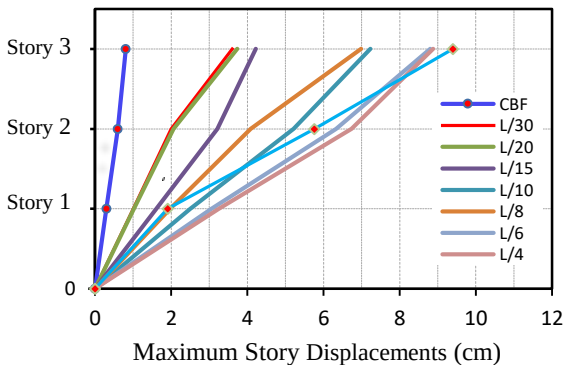

(e) Drift curves for 3 story frames (f) maximum lateral displacement curve for 3 story frames

Fig. 7. Lateral displacement curves of studied 3, 6 and 9 story frames

It should be noted that in table 1 to 3, the value of response modification factor for special concentrically braced frames (SCBFs) and concentrically braced frames braced with CSBs are set to be 5.5 and the response modification factor for intermediate SMFs is set to be 5. It should be taken into consideration that although there is no value for response modification factors of concentrically braced frames braced with CSBs in 2800 standard and ASCE 7, in this part of paper, their response modification factor is assumed to be 5.5 just like SCBFs, however in the next section, the validity of this assumption will be evaluated.

As it is displayed in tables 1 to 3 and Figure 7, as the value of ξ increases, maximum lateral displacement and period of concentrically braced frames braced with CSBs increases too, and for ξ =L/5 their behavior is just like intermediate steel intermediate moment-resisting frames.

According to figure 7, the strength and lateral stiffness of concentrically braced frames braced with CSBs are not coupled because as the value of ξ increases the lateral stiffness of the frame significantly decreases, so that for ξ>L/4 the lateral stiffness of them is even less than moment resisting frames' lateral stiffness, in other words, for ξ>L/4 the maximum lateral displacement of concentrically braced frames braced with CSBs is even more than moment-resisting frames, although decrease of lateral stiffness is not so appropriate but by setting ξ to proper value, desired strength and stiffness can be achievable. Figure 8 displays material used in studied frames.

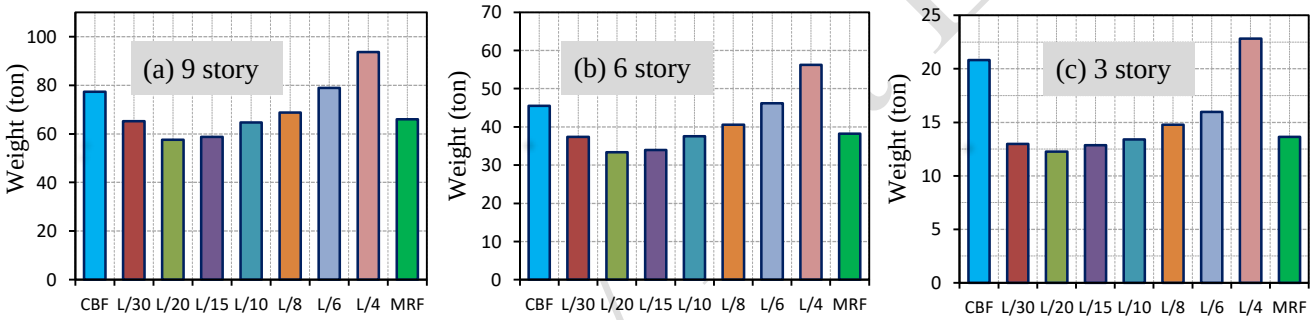

Fig. 8. Used steel curve for 3, 6, and 9 story studied frames

As observed from the curve in Figure 8, the amount of steel consumption increases with an increase in the value of ξ, however for ξ between L/20 and L/15, the amount of steel consumption has the minimum amount.

4. Evaluating ductility of concentrically braced frames braced with CSBs

After evaluating elastic responses of concentrically braced frames braced with CSBs, maximum ductility of them, is another problem that this paper deals with, in other words, it should be identified whether or not that concentrically braced frames braced with CSBs, can meet the proposed ductility of design guidelines or not. And if the desired ductility is guaranteed by concentrically braced frames braced with CSBs, for which value of ξ the maximum ductility can be obtained.

In most of seismic design guidelines, the ratio of maximum displacement to yield displacement is known as ductility and can be obtained using following equation:

$$\mu = \frac{\delta_u}{\delta_{yeff}} \qquad (5)$$

Also, according to FEMA P695 [FEMA P695, 2009], the value of over strength factor and corresponding *yield* displacement (δ_{yeff}) can be obtained from the following equation and using Figure 9:

$$\Omega = \frac{V_{max}}{V_{des}} \qquad (6)$$

$$\delta_{yeff} = C_0 \frac{V_{max}}{W}\left(\frac{g}{4\pi^2}\right)[\max(T, T_1)]^2 \qquad (7)$$

Where: C_0 is fundamental-mode displacement to roof displacement and according to FEMA P695 its value for a 3 story frames is ½ and for 6 and 9 story frames is 1/3, $\frac{V_{max}}{W}$ is the ratio of maximum base shear to weight of structure, g is the gravity constant, T is the fundamental period which is obtained from experimental equations (proposed by designing specification) and T_1 is the fundamental period of archetype model computed using eigenvalue analysis.

Also based on the Newmark and Hall [Newmark and Hall, 1982] method the force reduction factor due to ductility of structure can be calculated using the following equation:

$$R_\mu = \begin{cases} 1 & T \le 0.33\,\text{sec} \\ \sqrt{2\mu - 1} & 0.12 < T < 0.5\,\text{sec} \\ \mu & T > 1\,\text{sec} \end{cases} \quad (8)$$

And finally, the response modification factor can be obtained using equation 9:

$$R = \Omega \times R_\mu \quad (9)$$

To determine the seismic parameters (R, R_μ, Ω, μ) for the studied frames in this research, a nonlinear static analysis method (pushover analysis) has been employed. The foundation of this method is based on performing a series of step-by-step analyses. In each step of this analysis, the reduction in member stiffness due to the formation of plastic hinges is considered, along with the nonlinear behavior curve of the members at predetermined points. In this study, for pushover analysis, the lateral load pattern follows the same distribution as the earthquake force in the height of the frames. Additionally, the nonlinear behavior of seismic members is modeled using the behavior curve provided in FEMA 356 [FEMA 356, 2000] guidelines (Figure 9).

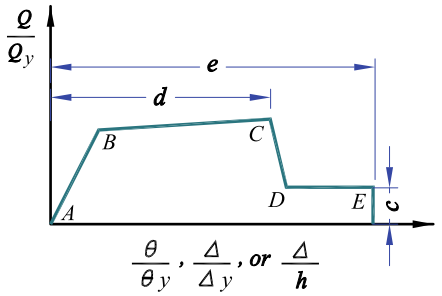

Fig. 9. Deformation curve of members [40]

Figures 10, 11 and 12 display the capacity curve and tables 4, 5 and 6 display seismic parameters of studied frames.

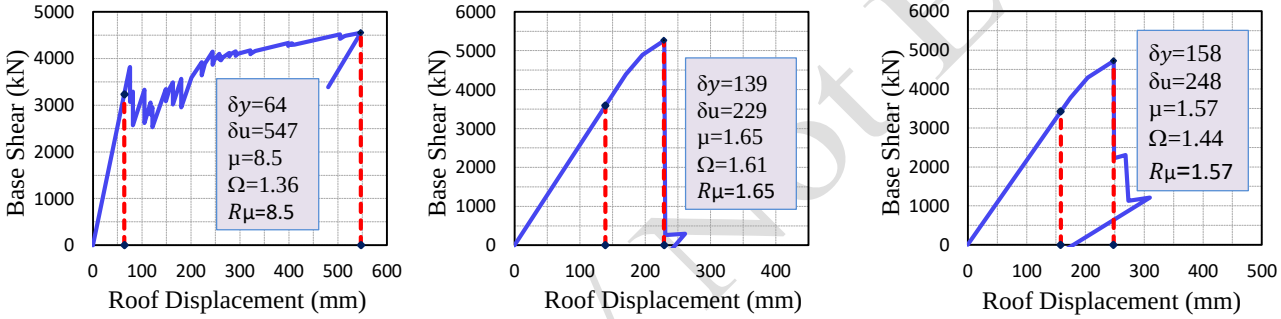

(a) 9 Story and ξ =0 (b) 9 Story and ξ =L/20 (c) 9 Story and ξ =L/15

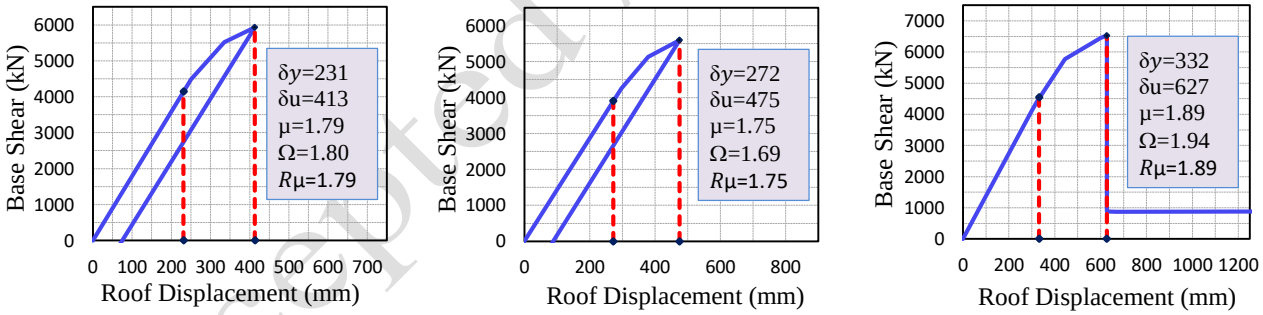

(d) 9 Story and ξ =L/10 (e) 9 Story and ξ =L/8 (f) 9 Story and ξ =L/6

Fig. 10. Capacity curves of 9 story braced frames

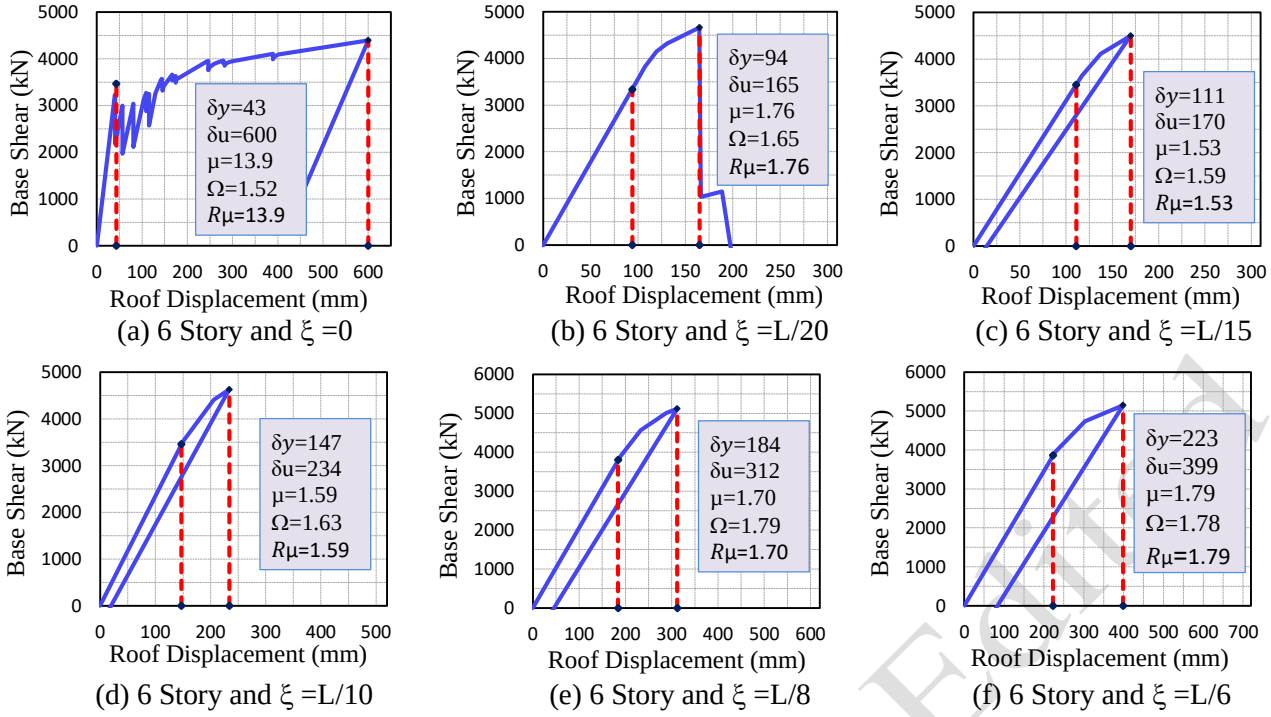

(a) 6 Story and ξ =0 (b) 6 Story and ξ =L/20 (c) 6 Story and ξ =L/15

(d) 6 Story and ξ =L/10 (e) 6 Story and ξ =L/8 (f) 6 Story and ξ =L/6

Fig. 11. Capacity curves of 6 story braced frames.

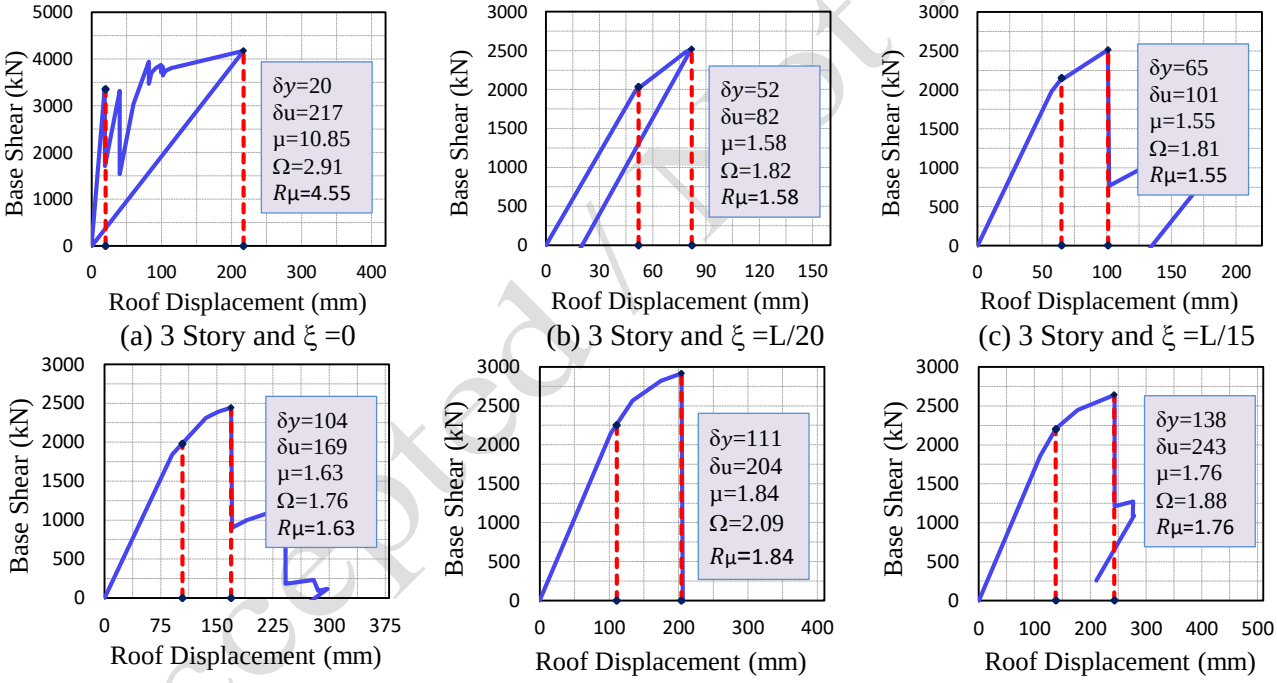

(a) 3 Story and ξ =0 (b) 3 Story and ξ =L/20 (c) 3 Story and ξ =L/15

(d) 3 Story and ξ =L/10 (e) 3 Story and ξ =L/8 (f) 3 Story and ξ =L/6

Fig. 12. Capacity curves of 3 story braced frames

Table 4. Nonlinear analysis results of 9 story studied frames

Type of Frame	V_{des} (kN)	V_{max} (kN)	δ_{yeff} (mm)	δ_u (mm)	W (kN)	C_0	T (sec)	T_1 (sec)	μ	Ω	R_μ	R
CBF	3355	4546	64	547	27661	1.3	0.679	1.098	8.5	1.36	8.5	11.56
ξ = L/30	3301	5460	136	229	27217	"	"	1.446	1.68	1.65	1.68	2.77
ξ = L/20	3266	5262	139	229	26924	"	"	1.481	1.65	1.61	1.65	2.66
ξ = L/15	3271	4719	158	248	26965	"	"	1.673	1.57	1.44	1.57	2.26
ξ = L/10	3299	5930	231	413	27194	"	"	1.809	1.79	1.80	1.79	3.22
ξ = L/8	3317	5593	272	475	27345	"	"	2.029	1.75	1.69	1.75	2.96
ξ = L/6	3364	6526	332	627	27733	"	"	2.102	1.89	1.94	1.89	3.67
ξ = L/4	3431	6008	411	713	28289	"	"	2.448	1.74	1.75	1.74	3.05
MRF	2451	5082	417	1212	27237	"	1.0864	2.629	2.91	2.07	2.91	6.02

Table 5. Nonlinear analysis results of 6 story studied frames

Type of Frame	V_{des} (kN)	V_{max} (kN)	δ_{yeff} (mm)	δ_u (mm)	W (kN)	C_0	T (sec)	T_1 (sec)	μ	Ω	R_μ	R
CBF	2890	4394	43	600	18200	1.3	0.5010	0.743	13.95	1.52	13.95	21.20
$\xi = L/30$	2844	4863	94	168	17908	"	"	1.033	1.79	1.71	1.79	3.06
$\xi = L/20$	2820	4656	94	165	17756	"	"	1.054	1.76	1.65	1.76	2.90
$\xi = L/15$	2823	4500	111	170	17778	"	"	1.167	1.53	1.59	1.53	2.43
$\xi = L/10$	2844	4628	147	234	17909	"	"	1.327	1.59	1.63	1.59	2.59
$\xi = L/8$	2863	5113	184	312	18026	"	"	1.418	1.70	1.79	1.70	3.04
$\xi = L/6$	2895	5151	223	399	18230	"	"	1.562	1.79	1.78	1.79	3.19
$\xi = L/4$	2956	5380	297	508	18613	"	"	1.782	1.71	1.82	1.71	3.11
MRF	2072	4258	271	619	17911	"	0.8015	1.880	2.28	2.06	2.28	4.70

Table 6. Nonlinear analysis results of 3 story studied frames

Type of Frame	V_{des} (kN)	V_{max} (kN)	δ_{yeff} (mm)	δ_u (mm)	W (kN)	C_0	T (sec)	T_1 (sec)	μ	Ω	R_μ	R
CBF	1434	4176	20	217	9014	1.2	0.2979	0.376	10.85	2.91	4.55	13.24
$\xi = L/30$	1389	2606	52	85	8731	"	"	0.767	1.64	1.88	1.64	3.08
$\xi = L/20$	1385	2517	52	82	8706	"	"	0.773	1.58	1.82	1.58	2.88
$\xi = L/15$	1389	2516	65	101	8727	"	"	0.868	1.55	1.81	1.55	2.81
$\xi = L/10$	1391	2442	104	169	8744	"	"	1.119	1.63	1.76	1.63	2.87
$\xi = L/8$	1399	2917	111	204	8795	"	"	1.061	1.84	2.09	1.84	3.85
$\xi = L/6$	1405	2642	138	243	8834	"	"	1.244	1.76	1.88	1.76	3.31
$\xi = L/4$	1446	3611	180	329	9090	"	"	1.233	1.83	2.50	1.83	4.58
MRF	1522	2895	136	380	8698	"	0.4766	1.171	2.79	1.907	2.79	5.30

5. Non-linear modeling verification

To validate the accuracy of the nonlinear numerical modeling, we utilize the experimental test results of elliptic-braced steel frames available in Figure 14 conducted by Ghasemi et al [Jouneghani and Haghollahi, 2020a; Jouneghani and Haghollahi, 2020b]. A quasi-static cyclic test was performed following the ATC-24 loading protocol. A comparison of the force-deformation curves obtained from both the experimental tests and the numerical modeling demonstrates a high level of accuracy in the results which can be seen in Figure 13.

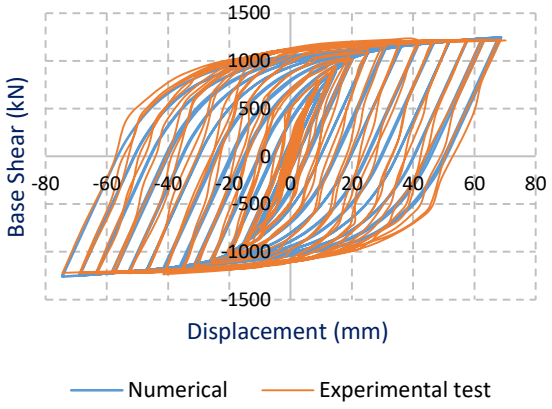

Fig. 13. Non-linear modeling verification

Fig. 14. Tests on elliptic-braced frames [41-42]

6. Evaluating cyclic behavior

During an earthquake, the structural loading is cyclic, therefore, using monotonic loading to investigate the non-linear behavior of the structure and its elements is inadequate, as it fails to account for crucial parameters such as stiffness reduction and strength degradation in ductility. To properly investigate the hysteresis behavior of the frame braced with CSBs, the ATC-24 loading protocol—shown in Figures 15 and 16—was employed for the beam-column connections.

According to ATC-24, n_0 is the number of cycles with peak deformation less than δ_y and is recommended to be less than 6; n_1 is the number of cycles with peak deformation equal to δ_y and is recommended to be less than 3, n_2 the number of cycles with peak deformation less than $\delta_2 = \delta_y +$

Δ and is recommended to be at least 3 unless a lower number can be justified. n_3 the number of cycles with peak deformation less than $\delta_2 = \delta_y + 2\Delta$ and is recommended to be at least 3 unless a lower number can be justified. n_4 to n_m the number of cycles with peak deformation less than $\delta_2 = \delta_y + 3\Delta$ to $\delta_m = \delta_y + (m-1)\Delta$ and is recommended to be at least 2 unless a lower number can be justified.

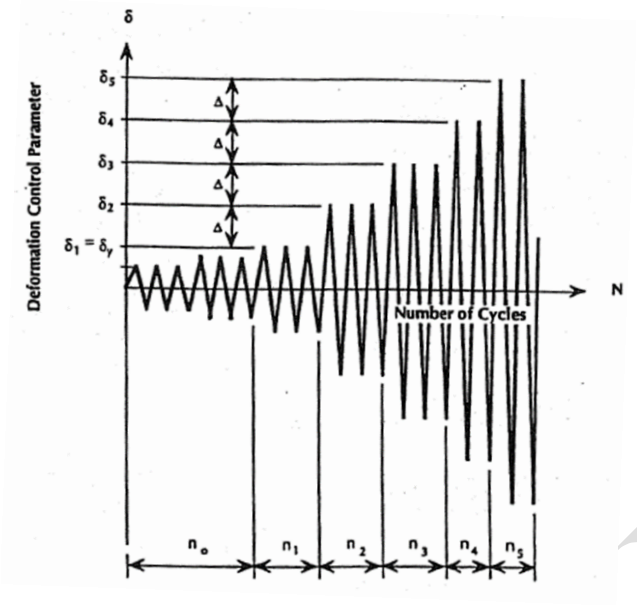

Fig. 15. ATC 24 cyclic loading protocol

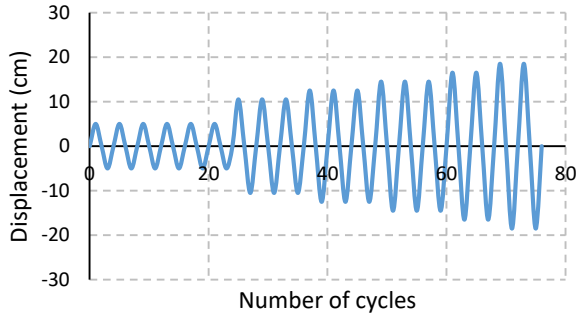

Fig. 16. protocol used for studied frames

As Figure 17 displays, hysteretic behavior of the 3-story frame which were indicated in previous sections, is obtained using opensees which is an open-source software for modeling nonlinear behavior of structures, as it is displayed in the graphs using CSB leads to more energy dissipations and the area under the hysteresis diagram increases as the ξ increases. And better hysteresis behavior can be achieved. It is acknowledged that while the cyclic behavior of frames equipped with CSBs was assessed using cyclic pushover protocols (ATC-24), further comprehensive evaluation through nonlinear time history analyses (NLTHA) using real earthquake ground motions is recommended for future studies to capture the full dynamic response and validate the findings under realistic seismic conditions.

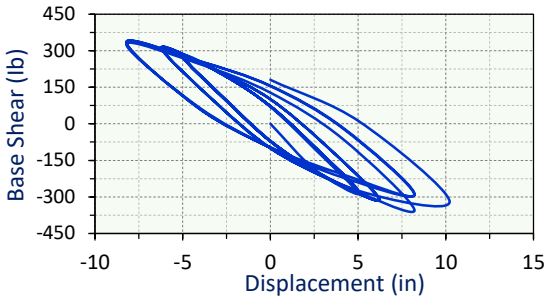

(a) 3-story moment resisting frame

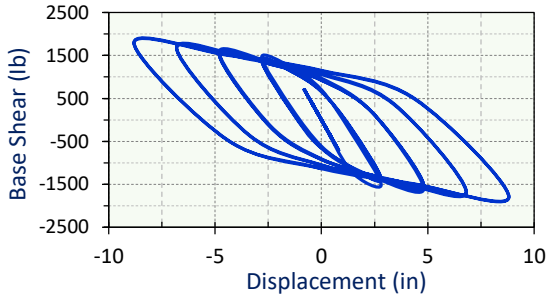

(b) 3-story concenrically braced frame

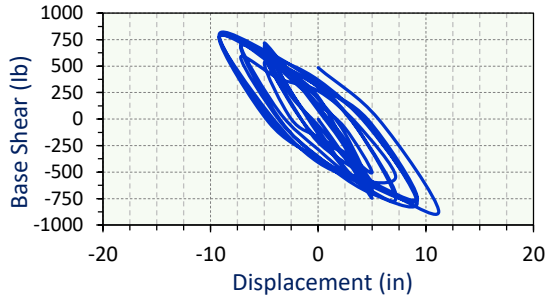

(c) 3-story crescent shape braces ($\xi = L/4$)

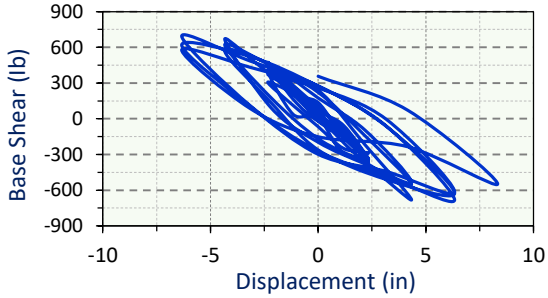

(d) 3-story crescent shape braces ($\xi = L/6$)

Fig. 17. hysteretic curves of 3-story frames

7. Discussion

Evaluation of elastic behavior of concentrically braced frames equipped with CSBs, in section 2, identified that for these frames, stiffness and strength of braced members are not coupled. The required strength and stiffness can be achieved by adjusting the value of ξ. However this feature is not available in common bracings where stiffness and

strength are coupled. It was also confirmed that by increasing the value of ξ, the frame's lateral stiffness reduces significantly, even if the bracing members have enough strength to withstand seismic forces. Additionally, it was confirmed that when ξ= L/5, the lateral stiffness of these frames is the same as that of moment-resistant frames.

Although based on the content presented in section 2.2, it appears that the ductility of this type of structural frame increases with an increase in the value of ξ. However, according to the results shown in Figures 11 to 12 and 17 and also based on the results presented in Tables 4 to 6, it is observed that with an increase in the value of ξ, not only a significant change in the seismic parameters (R, R_μ, Ω, μ) is not achieved, but fundamentally, in these types of structural frames, even if supplementary seismic requirements are met, the necessary ductility is not provided. In other words, if crescent shaped bracing members are used in structural frames (with hinge connections between beams and columns), and their design is based on R=5.5, then according to the results shown in Tables 4 to 6, the calculated response modification factor for all these frames is consistently less than 5.5, and the required ductility is not achieved. Figure 18 displays response modification factor curve of studied SCBFs, concentrically braced frames braced with CSBs, and intermediate steel moment resisting frames.

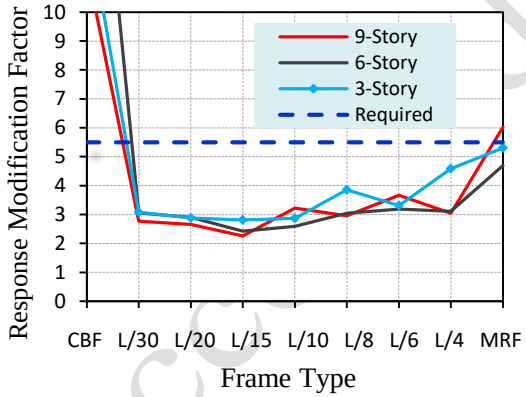

Fig. 18. Response modification factor change based on used ξ

Figure 18, illustrates that concentrically braced frames braced with CSBs can't be categorized as SCBFs, because their response modification factor is always lower than 5.5, also Figure 18, confirms that concentrically braced frames braced with CSBs can be categorized as OCBFs because the required response modification factor for OCBFs is the same as concentrically braced frames braced with CSBs and it can be achievable easily in these frames, this should be noted that in this study concentrically braced frames braced with CSBs are designed with R=5.5, so if they had been designed using R=3.5, then the values of response modification factors would be higher than the values which are presented in Figure 18, so as a result, required response modification factor of concentrically braced frames braced with CSBs can be easily achieved.

One of the reasons that concentrically braced frames braced with CSBs could not achieved the required response modification factor of SCBFs is because of plastic hinge formation, as it can be understood from Figure 19, which displays one of failure mechanisms of concentrically braced frames braced with CSBs, in these frames as the plastic hinges are formed in the middle of some of braces, some other plastic hinges are formed adjacent to initial plastic hinges, this leads to increase of deformation prior to plastic hinge formation in other stories' bracing members and according to curves proposed by FEMA 356, strength loss accrues and the pushover curve stops, so this can be one of the weak points of concentrically braced frames braced with CSBs for their inelastic responses, however it seems if CSBs are used in dual systems (moment resisting frame plus CSBs), then the dual system's required response modification factor can be improved by adjusting the value of ξ.

Furthermore, based on the sequence of plastic hinge formation observed during the analysis, as illustrated in Figure 19, it is evident that plastic hinges do not develop in the columns or beams before forming in the braces. This confirms the effectiveness of the capacity-limited design, ensuring that the braces function as structural fuses.

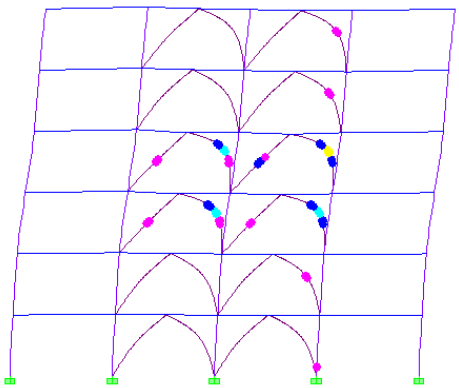

Fig 19. Failure mechanism of a 6-story building frame braced with CSBs for $\xi = L/10$

8. Conclusion

Crescent-shaped braces are novel and innovative seismic-resistant systems that allow for the adjustment of strength and stiffness by varying the value of ξ. In this research, several numerical models with different values of ξ are investigated to

evaluate the seismic performance of these systems. The main conclusions of this study are as follows:

1- For concentrically braced frames equipped with CSBs, stiffness and strength are not coupled. The required strength and stiffness can be achieved by adjusting the value of ξ.
2- By increasing the value of ξ, the lateral stiffness of concentrically braced frames equipped with CSBs decreases significantly. The stiffness ratio of CSBs to CBF decreases from approximately 0.41 to 0.03 as ξ varies from L/30 to L/4.
3- Lateral stiffness of concentrically braced frames equipped with CSBs is the same as moment-resisting frames when ξ is about L/5.
4- The maximum story drift in all studied frames remains below 0.023 during the elastic analysis.
5- For the studied 3-, 6-, and 9-story frames, the utilized steel weight is minimized at ξ = L/20 and maximized at ξ = L/4.
6- For concentrically braced frames equipped with CSBs, required ductility cannot be achieved even with complementary seismic provisions. In other words, if CSBs are used with frames with column-beam simple hinged connections and designed based on R=5.5, push-over analysis indicates the calculated response modification factor is always lower than 5.5, and the required ductility cannot be achieved.
7- Concentrically braced frames equipped with CSBs are categorized as OCBFs, and their response modification factor should be 3.5.

References

AISC A (2022) AISC 341-22. Seismic provisions for structural steel buildings. Chicago (IL): *American Institute of Steel Construction*.

Asghari, A., & Azimi, B. (2017). Evaluation of sensitivity of CBFs for types of bracing and story numbers. *Scientia Iranica*, 24(1), 40-52. https://dx.doi.org/10.24200/sci.2017.2375

Asghari, A., & Azimi Zarnagh, B. (2017). A new study of seismic behavior of perforated coupled shear walls. *International Journal of Civil Engineering*, 15, 775-789. https://doi.org/10.1007/s40999-017-0174-y

Asghari, A., & Gandomi, A. H. (2016). Ductility reduction factor and collapse mechanism evaluation of a new steel knee braced frame. *Structure and Infrastructure Engineering*, 12(2), 239-255. https://doi.org/10.1080/15732479.2015.1009123

Asghari, A., & Saharkhizan, S. (2019). Seismic design and performance evaluation of steel frames with knee-element connections. *Journal of Constructional Steel Research*, 154, 161-176. https://doi.org/10.1016/j.jcsr.2018.11.011

Asghari, A. (2016a). Evaluating the Ductility of X-braced Frames which are Braced in two Middle Adjacent Spans. *Ferdowsi Civil Engineering*, 27(2), 57-74. https://dx.doi.org/10.22067/civil.v27i2.33325

Asghari, A. (2016b). Ductility reduction factor evaluation of combined inverted v-braced and v-braced frames. *Sharif Journal of Civil Engineering*, 32-2(2.1), 101-110. https://www.sid.ir/en/journal/viewpaper.aspx?id=525899

Asghari, A. (2017). Evaluation of Ductility Reduction Factor for X-braced Steel Frames Which are Braced in Two End spans. *Amirkabir Journal of Civil Engineering*, 49(2), 213-226. https://www.sid.ir/en/journal/viewpaper.aspx?id=572678

Asghari, A. & Asadi, H. (2016). Seismic design of building frames in conjunction with concentric braces using the temperature variation method in braced members. *Sharif Journal of Civil Engineering*, 32(1.2), 109-118. https://www.sid.ir/en/journal/viewpaper.aspx?id=513723

Aydin, E., Ozturk, B., & Duzel, E. (2012). Rehabilitation of planar building structures using steel diagonal braces and dampers. *rehabilitation*, 16(17), 18.

Aydin, E., Ozturk, B., & Sahin, E. Investigation of Behavior of Adjacent Planar Steel Frames Connected with Rigid Bars under Earthquake Effects.

Aydin, E., Öztürk, B., & Dutkiewicz, M. (2019). Analysis of efficiency of passive dampers in multistorey buildings. *Journal of Sound and Vibration*, 439, 17-28. https://doi.org/10.1016/j.jsv.2018.09.031

Bastami, M., & Jazany, R. A. (2019). Development of centrically fused braced frame (CFBF) for seismic regions. *Soil Dynamics and Earthquake Engineering*, 127, 105856. https://doi.org/10.1016/j.soildyn.2019.105856

Bypour, M., Mahmoudian, A., Tajik, N., Taleshi, M. M., Mirghaderi, S. R., & Yekrangnia, M. (2024). Shear capacity assessment of perforated steel plate shear wall based on the combination of verified finite element analysis, machine learning, and gene expression programming. *Asian Journal of Civil Engineering*, 25(7), 5317-5333. https://doi.org/10.1007/s42107-024-01115-8

ETABS (1995), Integrated building design software, nonlinear version 9.7.3, Berkeley; California, USA

Fanaie, N., Mohammadzade, B., Gharebaghi, S. A., & Sarkhosh, O. S. (2024).

Design procedure of a shear fuse system for steel moment-resisting frames. *In Structures* (Vol. 63, p. 106473). Elsevier. https://doi.org/10.1016/j.istruc.2024.106473

FEMA 356 (2000) Commentary for the seismic rehabilitation of buildings. *FEMA 356, Federal Emergency Management Agency*, Washington, DC.

FEMA P695 (2009), Quantification of seismic performance factors, *FEMA P695 report, prepared by the Applied Technology Council for the Federal Emergency Management Agency*. Washington, DC.

Iranian code of practice for seismic resistant design of buildings. *Standard 2800*.

Izadinia, M., Rahgozar, M. A., & Mohammadrezaei, O. (2012). Response modification factor for steel moment-resisting frames by different pushover analysis methods. *Journal of Constructional Steel Research*, 79, 83-90. https://doi.org/10.1016/j.jcsr.2012.07.010

Jaberi, V., Asghari, A. (2020a). Evaluation of seismic response of linked column with simple frame system. *Modares Civil Engineering journal*, 23,19,6.41-58. https://mcej.modares.ac.ir/article-16-31002-en.html

Jaberi, V., & Asghari, A. (2020b). Seismic rehabilitation of existing buildings by linked column system. *Sharif Journal of Civil Engineering*, 36(3.1), 55-65. https://dx.doi.org/10.24200/j30.2019.52748.2504

Jaberi, V., & Asghari, A. (2022). Seismic behavior of linked column system as a steel lateral force resisting system. *Journal of Constructional Steel Research*, 196, 107428. https://doi.org/10.1016/j.jcsr.2022.107428

Jaberi, V., Jaberi, M., & Asghari, A. (2024). A new performance-based seismic design method using endurance time analysis for linked column frame system and a comparison of structural systems and seismic analysis methods. *The Structural Design of Tall and Special Buildings*, 33(10), e2100. https://doi.org/10.1002/tal.2100

Jalilzadeh Afshari, M., Asghari, A., & Gholhaki, M. (2019). Shear strength and stiffness enhancement of cross-stiffened steel plate shear walls. *International Journal of Advanced Structural Engineering*, 11(2), 179-193. https://doi.org/10.1007/s40091-019-0224-6

Jouneghani, H. G., & Haghollahi, A. (2020a). Experimental and analytical study in determining the seismic performance of the ELBRF-E and ELBRF-B braced frames. *Steel and Composite Structures*, 37(5), 571-587. https://doi.org/10.12989/scs.2020.37.5.571

Jouneghani, H. G., & Haghollahi, A. (2020b). Experimental study on hysteretic behavior of steel moment frame equipped with elliptical brace. *Steel Compos Struct*, 34(6), 891-907. https://doi.org/10.12989/scs.2020.34.6.891

Mahmoudian, A., Tajik, N., Darabi, A., Mohammadzadeh Taleshi, M., Marmarchinia, S., Asghari, A., & Mirghaderi, S. R. (2024). Integrating machine learning and genetic expression programming for enhanced punching shear strength prediction. *Civil Engineering Infrastructures Journal*. https://doi.org/10.22059/ceij.2024.380171.2118

Mesr Habiby, Y., & Behnamfar, F. (2023). Seismic fragility analysis of torsionally-coupled steel moment frames against collapse. *Civil Engineering Infrastructures Journal*, 56(2), 415-438. https://doi.org/10.22059/ceij.2023.347246.1862

Mohammadgholipour, A., & Billah, A. M. (2024). Performance-based plastic design and seismic fragility assessment for chevron braced steel frames considering aftershock effects. *Soil Dynamics and Earthquake Engineering*, 178, 108440. https://doi.org/10.1016/j.soildyn.2023.108440

Newmark, N. M., & Hall, W. J. (1982). Earthquake spectra and design. *Engineering monographs on earthquake criteria*.

Palermo, M., Silvestri, S., Gasparini, G., & Trombetti, T. (2015). Crescent shaped braces for the seismic design of building structures. *Materials and Structures*, 48, 1485-1502. https://doi.org/10.1617/s11527-014-0249-z

Rezaee, M., & Asghari, A. (2024, October). Lateral-torsional buckling investigation of multi-tiers eccentrically braced frames with shear link beam. *In Structures* (Vol. 68, p. 107063). Elsevier. https://doi.org/10.1016/j.istruc.2024.107063

Sabelli R. (2001), "Research on improving the seismic behavior of earthquake-resistant steel braced frames". EERI/FEMA NEHRP Professional Fellowship Rep. *Earthquake Engineering Research Institute*, Oakland, CA.

Shirpour, A., Fanaie, N., & Seraji, M. B. (2024). Seismic performance factors of quarter-elliptic-braced steel moment frames (QEB-MFs) using FEMA P695 methodology. *Soil Dynamics and Earthquake Engineering*, 178, 108453. https://doi.org/10.1016/j.soildyn.2024.108453

Shirpour, A., & Fanaie, N. (2024). Quantifying the seismic performance factors of half-elliptic-braced steel moment frames (HEB-MFs). *Engineering Structures*, 311, 118189. https://doi.org/10.1016/j.engstruct.2024.118189

Steneker, P., Filiatrault, A., Wiebe, L., & Konstantinidis, D. (2020). Integrated structural–nonstructural performance-based seismic design and retrofit optimization of buildings. *Journal of Structural Engineering*, 146(8), 04020141. https://doi.org/10.1061/(ASCE)ST.1943-541X.0002680

Tajik, N., Marmarchinia, S., Mahmoudian, A., Asghari, A., & Mirghaderi, S. R. (2025a). The effect of multi-pass welding on residual stresses in fillet welded built-up steel box sections. *Asian Journal of Civil Engineering*, 26(2), 955-974. https://doi.org/10.1007/s42107-024-01218-2

Tajik, N., Mirghaderi, S. R., & Asghari, A. (2025b). Comparative Numerical Analysis of Residual Stresses in Fillet and CJP Welded Built-Up Steel Box-Shaped Columns. *Journal of Structural Design and Construction Practice*, 30(3), 04025032. https://doi.org/10.1061/JSDCCC.SCENG-1665

Tajik, N., Mirghaderi, S. R., Asghari, A., & Hamidia, M. (2024). Experimental and numerical study on weld strengths of built-up steel box columns. *Journal of Constructional Steel Research*, 213, 108362. https://doi.org/10.1016/j.jcsr.2023.108362

Tajik, N., Mirghaderi, S. R., Asghari, A., & Hamidia, M. (2025c). Experimental and numerical evaluation of weld strengths in steel box columns under bending and combined forces. *Journal of Constructional Steel Research*, 226, 109195. https://doi.org/10.1016/j.jcsr.2024.109195

Wang, C. L., Gao, Y., Cheng, X., Zeng, B., & Zhao, S. (2019). Experimental investigation on H-section buckling-restrained braces with partially restrained flange. *Engineering Structures*, 199, 109584. https://doi.org/10.1016/j.engstruct.2019.109584

Yuan, Y., Gao, J., Qing, Y., & Wang, C. L. (2022). A new H-section buckling-restrained brace improved by movable steel blocks and stiffening ribs. *Journal of Building Engineering*, 45, 103650. https://doi.org/10.1016/j.jobe.2021.103650

Özuygur, A. R. (2016). Performance-based Seismic Design of an Irregular Tall Building—A Case Study. *In Structures* (Vol. 5, pp. 112-122). Elsevier. https://doi.org/10.1016/j.istruc.2015.10.001